I&EC research
Industrial & Engineering Chemistry Research

pubs.acs.org/IECR

Article

High-Temperature Conversion of Olefins to Liquid Hydrocarbons on γ-Al_2O_3

Matthew A. Conrad, Jaiden E. DeLine, and Jeffrey T. Miller*

Cite This: *Ind. Eng. Chem. Res.* 2023, 62, 4840−4850

Read Online

ACCESS | Metrics & More | Article Recommendations | Supporting Information

ABSTRACT: Noncatalytic thermal conversion of light olefins proceeds at industrially relevant rates at temperatures above 450 °C and pressures above 50 bar. The discovery of solid acid oligomerization catalysts permitted the use of milder conditions (<300 °C) and significantly improved the octane rating. However, Brønsted acid catalysts deactivate and must be regenerated frequently. In this study, at reaction temperatures of about 250−450 °C and pressures of 1 to 40 bar, olefins react on γ-alumina to form higher molecular weight products. The rate of propylene is about ten times higher than that of ethylene. The products, however, are not a simple olefin oligomerization distribution, and many nonoligomer products are formed. The primary products undergo secondary reactions, including double bond isomerization and H-transfer, giving moderate selectivities for saturated products. Depending on the conversion, temperature, and pressure, the rate of ethylene conversion on alumina is more than 100 times that of thermal, noncatalytic conversion. The apparent activation energy for ethylene conversion is 55−75 kJ/mol, which is much lower than ∼244 kJ/mol observed for the thermal gas-phase reaction. On alumina, some reactants and products undergo disproportionation reactions. For example, propylene forms equal molar amounts of ethylene and *iso*-butene even at very low conversions. Lewis acid sites on γ-alumina have previously been proposed as the active site for double bond isomerization and H−D exchange. Thus, it seems likely that Lewis acid sites are also catalytic for olefin oligomerization and disproportionation reactions. With the γ-alumina catalyst, high liquid yields can be achieved with little formation of coke and minimal deactivation for at least several days.

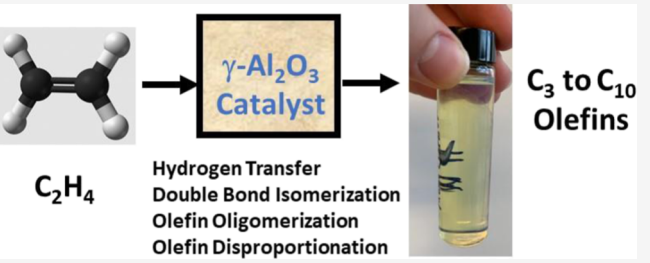

1. INTRODUCTION

Oligomerization of ethylene and propylene is an important upgrading reaction, such as in the valorization of the ethane and propane in shale gas into motor fuels or the production of sustainable aviation fuels from bioalcohol.[1−3] There are three broad classes of olefin oligomerization, catalysts depending on the type of reactive intermediate formed: carbanion-like species (organometallic or supported transition metal-alkyl catalysts),[4−14] carbenium ions (Brønsted acid catalysts),[13−21] and free radicals (thermal noncatalytic reactions).[15,22−29] The first two have been studied extensively over the past half-century, whereas the latter, which was discovered first, has been given little consideration since the 1950s.

Carbanionic-like, metal-alkyl oligomerization catalysts, for example, with nickel,[30−34] titanium,[35] chromium,[36,37] aluminum,[10,38] and zirconium,[39] convert ethylene either into linear, primary olefins (dimers, trimers, etc.) or nonselective (Schultz−Flory or Poisson) product distributions. These oligomer products are utilized as specialty chemicals but require additional transformations to become usable fuels. Homogeneous catalysts generally require co-catalyst activators and separation of the catalyst and products, spurring interest in heterogeneous transition-metal alternatives. The latter, however, have not been commercialized due to their comparatively lower productivity and/or rapid catalyst deactivation.

Brønsted acid, carbenium ion oligomerization is a common refinery operation to make motor fuels from cracked light olefins. The acidic catalysts can be liquid (e.g., H_3PO_4, H_2SO_4, and HF) or solid phase [e.g., solid phosphoric acid (SPA), zeolites, and resins].[13,15,20] Since liquid acids are corrosive and more hazardous, solid acid catalysts, such as SPA and zeolites, are preferred. Moreover, solid acid catalysts circumvent the need for expensive separations but are hindered by deactivation due to coking, site loss, and pore blockage, requiring frequent regeneration.

Thermal free-radical conversion of light olefins to liquids was the first refinery oligomerization process[23−25,40] yet did not experience widespread implementation due to the harsh temperatures required and relatively low octane rating

Received: August 1, 2022
Revised: February 27, 2023
Accepted: March 1, 2023
Published: March 13, 2023

https://doi.org/10.1021/acs.iecr.2c02759
Ind. Eng. Chem. Res. 2023, 62, 4840−4850

compared to SPA.[41] The detailed products and kinetic behaviors were recently delineated for the gas-phase, thermal radical reactions of ethylene, revealing that the C_4 and C_5 isomers by thermal oligomerization were mostly linear, terminal olefins.[42]

In this study, we investigate ethylene and propylene oligomerization over γ-alumina, which has been investigated for many other catalytic reactions.[43−59] Many studies have shown that pure alumina does not have Brønsted acidity but does contain multiple types of strong and weak Lewis acid sites.[59−62] Commercial processes using acidic alumina rely on the addition of chloride or fluoride ions, which confers Brønsted acidity.[63−66] Pure alumina is generally less active but has been demonstrated to catalyze hydrocarbon reactions: alcohol dehydration,[44,45,67] propane dehydrogenation,[58,59] ethylene hydrogenation,[49,50,53,68] olefin double bond and cis/trans isomerization,[47,48,52,54,55] and H_2-D_2 exchange of olefins and paraffins.[68−72] In addition, chemisorption experiments and infrared (IR) spectroscopy have provided evidence that ethylene forms chemically bonded intermediates at room temperature with alumina.[73] Silica, on the other hand, did not chemisorb ethylene.[74]

In this study, we address the following two questions:

1. Is alumina catalytic for olefin oligomerization of ethylene and propylene and what are the reaction conditions? What are the apparent kinetics for the oligomerization reactions?
2. What are the reaction products of ethylene and propylene over alumina? What reactions does alumina catalyze? What is the likely active site?

To determine the catalytic effect of γ-Al_2O_3 for olefin conversion, C_2H_4 conversion kinetics, for example, reaction rates, activation energies, reaction orders, and products, were measured from about 250 to 450 °C at 1.5 and 43 bar. The effects of ethylene conversion, reaction temperature, and pressure on the product distributions were also determined. High-surface-area, amorphous SiO_2 was also tested and compared to alumina. Silica has weakly acidic silanol (Si−OH) sites which are generally regarded as inert. In addition, propylene was also reacted with Al_2O_3 to better understand the product selectivity and, possibly, identify other secondary reaction pathways.

2. EXPERIMENTAL METHODS

2.1. Materials. Alumina (Al_2O_3). High-purity Catalox Sba 200 γ-alumina was obtained from Sasol, having a reported average pore size of 4−10 nm, a surface area of 200 m^2/g, and a pore volume of 0.35−0.5 cm^3/g. This alumina was in powder form, with an average size of 45 μm. The alumina was additionally characterized by Al MAS NMR and IR spectroscopy of adsorbed pyridine. Transmission IR spectra of adsorbed pyridine were collected using a Thermo Fisher Nicolet 4700 spectrometer equipped with a mercury cadmium telluride detector (MCT-A). Each spectrum was recorded by collecting 64 scans from 4000 to 650 cm^{-1} at a resolution of 2 cm^{-1}. Spectra were collected until surface equilibrium was achieved. Al_2O_3 was dehydrated at 300 °C prior to analysis at 150 °C. He was used to purge the sample of gas-phase pyridine at 150 °C (pure He, 50 mL/min) prior to data acquisition. The NMR spectrometer is a Chemagnetics CMX-400 with a wide-bore magnet and a Chemagnetics 5 mm H-X-Y triple-resonance MAS probe. For the ^{27}Al spectra, the parameters were as follows: 1-pulse acquisition with no ^{1}H decoupling, a pulse width of 2.3 μs (nominal P90 of ^{27}Al using a solution-state sample of 7 μs), a relaxation delay of 0.5 s, and an acquisition time of 25.6 ms. The sample rotation rate was 6 kHz, and 1k scans were typically acquired. The data were processed using a left-shift of two data points, exponential multiplication with a line-broadening of 100 Hz and one zero-fill.

Silica (SiO_2): High-purity grade (>99%) amorphous silica (Davisil 636) was purchased from Sigma-Aldrich, having an average pore diameter of 6.0 nm, a surface area of 480 m^2/g, and a pore volume of 0.75 cm^3/g. The particle size distribution was 200−500 μm (35−60 mesh).

2.2. Atmospheric Pressure Olefin Oligomerization. A quartz tube (10.5 mm ID, 1.1 mm thickness) of approximately 35 cm in total length was loaded into a clamshell furnace with insulation enclosing a 13 cm-long heated reaction zone. A thermal well placed down the axial length of the tube allowed the temperature profile to be measured at 2.5 cm intervals. A length-averaged temperature was then calculated for each temperature setpoint. The reactor was then heated to the desired setpoint and ethylene flow rate. For each data point, the product gas flow rate was verified using a bubble film flowmeter. Ultra-high-purity ethylene or propylene was purchased from Indiana Oxygen and used in all experiments.

Products were analyzed using a Hewlett Packard 6890 Series Gas Chromatograph with an Agilent HP-Al/S column (25 m in length, 0.32 mm ID, and 8 μm film thickness) and a flame ionization detector. The product peaks for C4 (isobutane and isobutene), C5 (*n*-pentane, isopentane, *n*-pentenes, and isopentenes), and C6 (1-hexene) isomers were identified by reference injections or inferred from known model reactions (e.g., the selective dehydrogenation of isopentane to isopentenes). To detect higher molecular weight products up to C8, the reactor discharge lines were traced with heat tape and set to 150 °C during the experiments. The conversion and product distribution were calculated on a molar basis, assuming a closed carbon balance since no significant carbon deposition was observed over the course of experiments.

2.3. High-Pressure Ethylene Oligomerization. To understand the product distributions and rates at higher olefin concentrations and conversions, ethylene was tested at pressures up to 43 bar. A 316 stainless steel tube (9.5 mm ID, 3.2 mm thickness) 60 cm in length, with VCR fittings at the inlet and outlet to seal the system, was used. The reactor setup was in a ventilated fume hood as a safety precaution, and a pressure relief valve rated for 45 bar was installed at the top of the reactor. The insulation allowed a thermal reaction zone of about 42 cm, which corresponded to a volume of ca. 30 cm^3. A thermal well placed down the length of the tube allowed the temperature profile to be measured at 5 cm intervals. A length-averaged temperature was then calculated for each temperature setpoint. The reactor was first pressurized to check for leaks, and then, it was heated to the desired setpoint temperature in flowing N_2 and allowed to stabilize for 4 h to purge oxygen from the system. Pure C_2H_4 was then flowed through the reactor. Ultra-high-purity ethylene, purchased from Indiana Oxygen, was used in all experiments.

Products were analyzed using a Hewlett Packard 7890 Series Gas Chromatograph with an Agilent HP-1 column (25 m in length, 0.32 mm ID, and 8 μm film thickness) and a flame ionization detector. To detect higher molecular weight products up to C10, the reactor discharge lines were traced

https://doi.org/10.1021/acs.iecr.2c02759
Ind. Eng. Chem. Res. 2023, 62, 4840−4850

with heat tape and set to 175 °C during the experiment. The conversion and product distribution were calculated on a molar basis, except at high conversions (X > 20%), in which the mass selectivity was more convenient to calculate due to the condensation of considerable amounts of liquid products, which were collected in a glass vial maintained in an ice bath. A comparison of the liquid production rate and unreacted ethylene in the gas effluent to the feed mass flow rate enabled an estimation of the conversion. For lower conversions (X < 20%), the product did not condense significantly. Additionally, little carbon deposition was observed over several days of testing; thus, a 100% carbon balance was assumed in the calculations.

3. RESULTS

3.1. Ethylene Reaction Rates, Kinetics, and Products with Alumina and Silica. For both silica and alumina, a higher ethylene conversion rate was observed compared to the gas-phase reaction at ca. 43 bar, shown in Table 1. The ethylene conversion rates were measured at 340 °C and olefin conversions below 5% using the PFR differential method. The conversions were compared relative to the gas hourly space velocity (GHSV), calculated as the thermal reaction volume divided by the gas volumetric flow rate. The thermal background conversion was subtracted from the products from alumina or silica. The conversion rate was about 600 times higher in the presence of Al_2O_3 but only 2.6 times higher in the presence of SiO_2. The gas-phase conversion was 0.082% at a GHSV of 8.0 h^{-1}, whereas with Al_2O_3, the conversion was 5.0% at a GHSV of 81 h^{-1}. With SiO_2, a GHSV of 5.4 h^{-1} resulted in 0.32% ethylene conversion. Alumina and silica were also compared by normalizing their surface areas (see Tables 1 and S1). The surface area was not responsible for the higher ethylene conversion rate. SiO_2 had a larger surface area per gram (480 m^2/g) compared to Al_2O_3 (200 m^2/g). However, Al_2O_3 had about 270 times higher conversion than SiO_2 per m^2.

Table 1. Comparison of Ethylene Conversion Rates at 340 °C and 43 bar C_2H_4

	GHSV (h^{-1})	conversion (%)	rate per surface area vs SiO_2	rate per volume vs thermal
thermal, gas phase	8.0	0.082		1
SiO_2	5.4	0.32	1	2.6
Al_2O_3	81	5.0	270	620

The presence of silica or alumina changed the kinetic parameters (reaction order and activation energy) compared to the thermal reaction, that is, the empty reactor. Estimates for the reaction order were made from the rate measurements at 1.5 and 43 bar at 340 °C by determining the slope of the ln(rate) versus the ln(P). The reaction orders for SiO_2, Al_2O_3, and thermal reactions were 1.4, 1.1, and 1.9, respectively (Table S2). Apparent activation energies were determined from 300 to 400 °C, at pressures of 1.5 and 43 bar, and ethylene conversions below 5%. Both silica and alumina also had lower apparent activation energies than the thermal reaction, which was 244 kJ/mol (Figure 1 and Table S2). The apparent activation energies for Al_2O_3 and SiO_2 were 55 and 89 kJ/mol, respectively, at 1.5 bar but increased at higher pressures, ca. 43 bar, to 76 and 176 kJ/mol. The activation energy of the thermal reaction did not change at higher pressure.

Silica and alumina both gave rise to similar molecular-weight (MW) distributions to those of the thermal reactions, with major differences occurring in the C4 and C5 isomer distributions with alumina. SiO_2 was reacted with ethylene at 360 °C and 43 bar, giving a conversion of 0.96%. For comparison, thermally, the conversion was 0.58%. The carbon number distributions, shown in Figure 2, are very similar for SiO_2 and the gas-phase reactions, and both oligomer and nonoligomer products, that is, odd carbon number olefins, are formed. In addition, the C4 linear isomer distributions in Figure 2b show that more double bond isomerization occurs with SiO_2 compared to gas-phase reactions, which produce about 80% 1-butene. With SiO_2, 1-butene is 44% of C4, with the remainder being mostly *trans*- and *cis*-2-butene. The

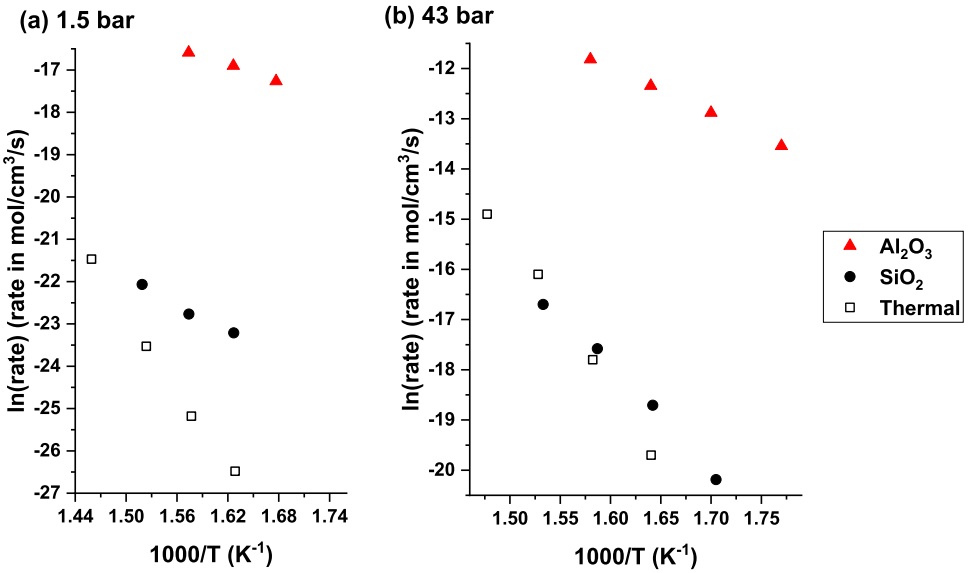

Figure 1. Kinetics of C_2H_4 reactions with alumina and silica and thermal reaction. Arrhenius plot from 300 to 410 °C at (a) 1.5 and (b) 43 bar C_2H_4. Apparent activation energies are given in Table S2.

https://doi.org/10.1021/acs.iecr.2c02759
Ind. Eng. Chem. Res. 2023, 62, 4840−4850

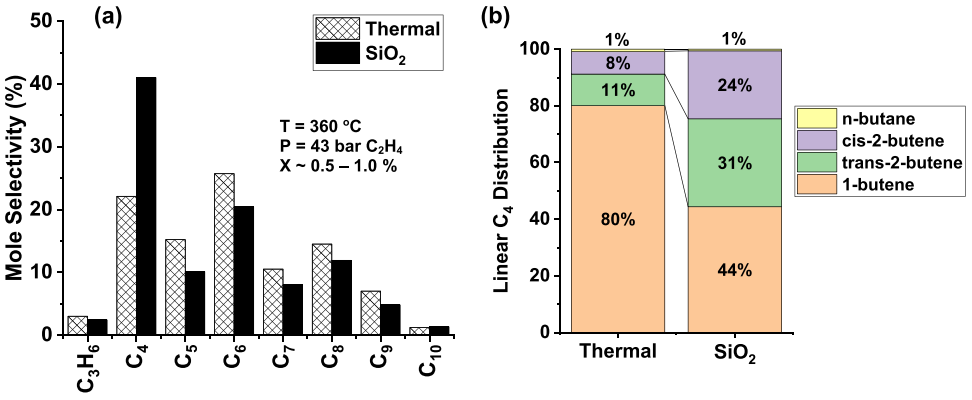

Figure 2. Products of ethylene conversion in the presence of SiO_2 compared to the thermal reaction at 360 °C, 43.0−43.5 bar. The conversions, both thermally and with SiO_2, were 0.58 and 0.96%, respectively. (a) Products based on carbon number distribution. (b) Linear C_4 distribution.

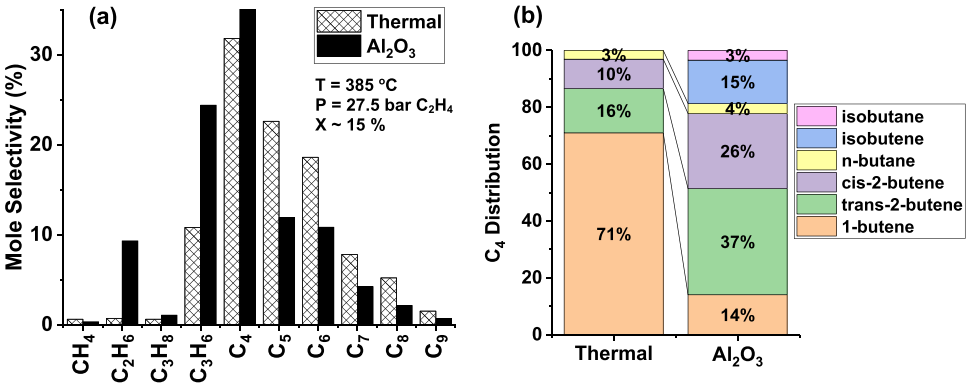

Figure 3. Products of ethylene conversion in the presence of alumina compared to the thermal reaction at 385 °C, 27.5 bar. The conversions, both thermally and with alumina, were 11.9 and 16.9%, respectively. (a) Products based on carbon number distribution. (b) Linear C_4 distribution.

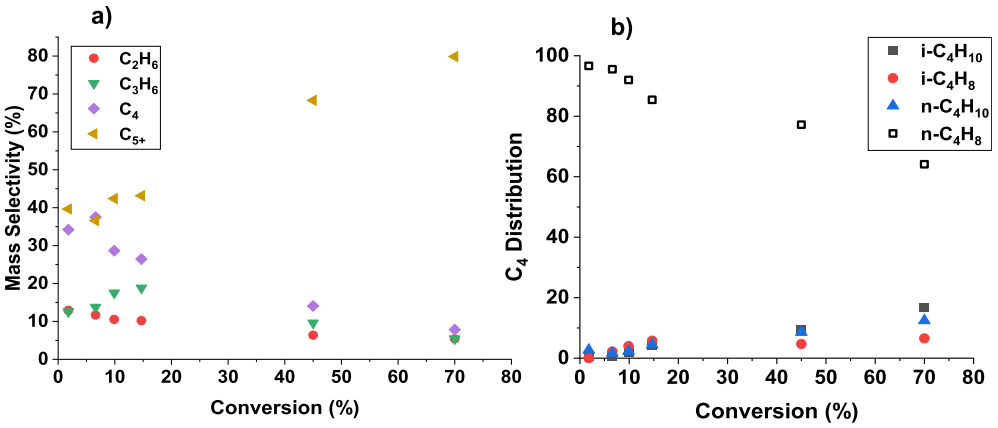

Figure 4. Products with Al_2O_3 at 23 bar C_2H_4, 360 °C, from 1 to 70% conversion. (a) Major products and (b) C_4 isomer distribution.

amount of *n*-butane is very small (ca. 1%) in both cases. Furthermore, there was no evidence of increased branched products such as isobutane or isobutene with silica.

For Al_2O_3, the most abundant products at these conditions are C4's, followed by propylene (35 and 25%, respectively). The remaining higher MW products (C_{5+}) decrease in the order of increasing carbon number. The same is true for the thermal reaction, except that there is less propylene and more C5 to C9 products. Thermally, C4 was the most abundant carbon number group (nearly 32%), while propylene was just 11%. The products for the alumina and thermal reactions shown in Figure 3 were measured at 385 °C and 27.5 bar, around 15% conversion. The two major differences observed between Al_2O_3 and the gas-phase reaction are the production of ethane and the C4 distribution. With Al_2O_3, there is about 9% selectivity to ethane, whereas in the thermal reaction, ethane is less than 1% of the products. In the C4 distribution for alumina, shown in Figure 3b, there is a significantly higher selectivity of branched C4 products, which were not observed in the thermal reactions of ethylene. Isobutene and *iso*-butane were collectively 18% of C4, and 1-butene was only 14% of C4. The remaining C4 were 2-butenes (63%). The gas-phase reaction produced 1-butene with 71% selectivity among C4 isomers.

https://doi.org/10.1021/acs.iecr.2c02759
Ind. Eng. Chem. Res. 2023, 62, 4840−4850

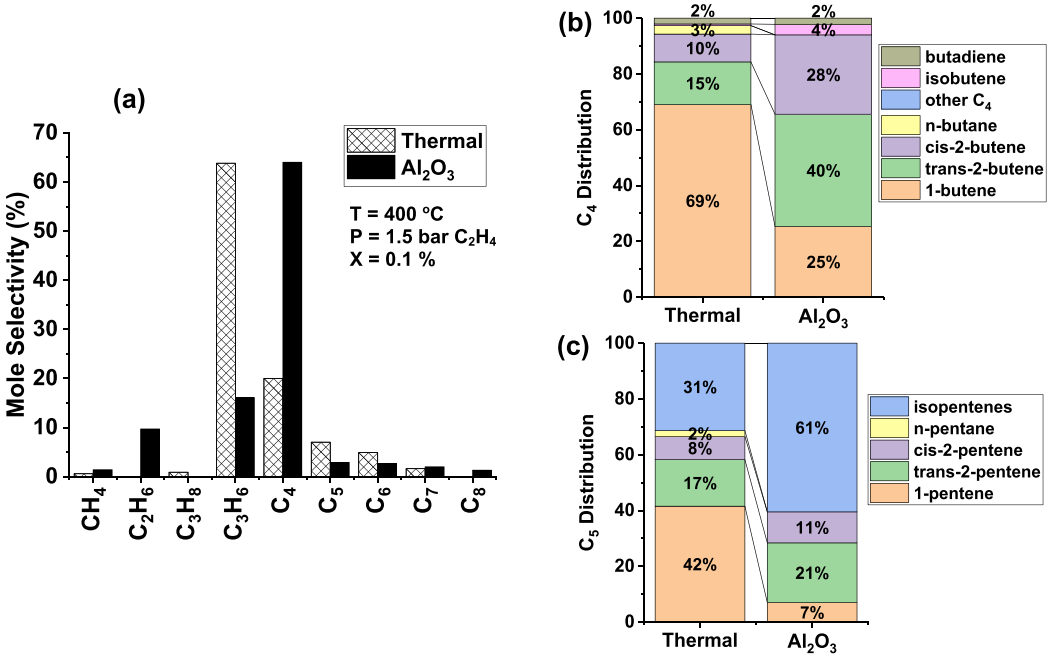

Figure 5. Products with Al_2O_3 vs the thermal reaction at 1.5 bar C_2H_4, 400 °C, and 0.1% conversion. (a) Carbon number distribution, (b) C_4 distribution, and (c) C_5 distribution.

In summary, the rate of ethylene oligomerization of Al_2O_3 is greater than 100 times that for the thermal reaction. In addition, the reaction order for ethylene decreases from second order for thermal reactions to first order on alumina. The activation energy also decreases from 254 kJ/mol for the former to 76−55 kJ/mol depending on the pressure for the latter. There were also differences in the product distributions. Al_2O_3 provided the best yield to desired C_{3+} products with significant branching of the C_{4+} hydrocarbons, whereas SiO_2 was not much different from the gas-phase reaction and formed mostly linear, terminal olefins. Therefore, reactions of ethylene and propylene on Al_2O_3 were studied over a wider range of conversion, temperature, and pressure conditions to better understand the reactions that occur on alumina.

3.2. Product Distribution at High Ethylene Conversion with Al_2O_3. At 360 °C and 23 bar, by varying the space velocity, ethylene conversions from 1 to 70% were obtained. High ethylene conversion on alumina produced C_{5+} liquid hydrocarbons with MW distributions similar to those of gas-phase reactions but at 100 °C lower temperature. At the same conditions, for example, temperature, pressure, flow rate, and reactor volume, the gas-phase conversion was less than 1% of the alumina conversion. The higher activity with alumina is consistent with the measured kinetic rates at lower pressure and is about 2 orders of magnitude higher than the thermal reaction. The MW distributions as a function of conversion in Figure 4 demonstrate the high selectivity to C_{5+} products. During this experiment, a light-yellow liquid product was condensed into an in-line vial submerged in an ice bath. The weight-hourly space velocity required to obtain 70% conversion was 0.1 h^{-1}. Approximately, 1 cm^3 of liquid hydrocarbons was condensed per hour during the 24 h duration of the trial. There was no apparent catalyst deactivation, at least, for several days. At the end of the experiment, Al_2O_3 in the center of the catalyst bed displayed a yellow-orange color but was not black, suggesting that coking was not significant at this temperature.

The major products were C_{5+}, C_4, propylene, and ethane, Figure 4. The methane selectivity was less than 1% at each conversion. The ethane selectivity decreased with increasing conversion, starting as high as 15 at 2% conversion, but becoming only about 5 at 70% conversion. Conversely, the C_{5+} products increased over the same conversion range from 40 to 80% of the products. The propylene and C_4 selectivities increase in the early stages of the reaction (below 20% conversion) but decrease at higher conversions.

3.3. Comparison of Products with Al_2O_3 versus the Thermal Reaction at Low Pressures and Conversions. The product distribution at low conversion (0.1%) at 400 °C and 1.5 bar reveals a slightly different MW distribution with alumina compared to the gas phase (Figure 5). The thermal conversion at the same volumetric flow rate was at least 50 times lower than for Al_2O_3. With Al_2O_3, the major products were 60% C_4, followed by 15% C_3H_6 and 10% ethane, in contrast to the gas phase, which produces 65% propylene, 20% C_4, and little ethane. Both the thermal reaction and Al_2O_3 produce less than 1.5% methane at this temperature. Along with propylene, nonoligomer products, such as C_5 and C_7, were present in comparable amounts to oligomers such as C_6 and C_8.

With alumina, there was a much higher selectivity for isomerized C_4 and C_5 products than for thermal reactions. For the former, the C_4 products were 68% 2-butenes and only 25% 1-butene, whereas for the latter, 1-butene was about 69%. Although the amount of isobutene produced is small (4%), it is nonetheless relatively higher than that produced without Al_2O_3 (<0.1%). Butadiene is also produced to a small extent in both cases (near 2%). No butane was observed with Al_2O_3, although about 3% selectivity was seen for thermal reactions, Figure 5b. The distribution of C_5 products with Al_2O_3 forms much less 1-pentene compared to double-bond and skeletal isomers. With Al_2O_3, 1-pentene selectivity was 7%, whereas the selectivities of isopentenes and 2-pentenes were 61 and 33%, respectively. In contrast, for the noncatalytic, thermal conversion, the C_5

https://doi.org/10.1021/acs.iecr.2c02759
Ind. Eng. Chem. Res. 2023, 62, 4840−4850

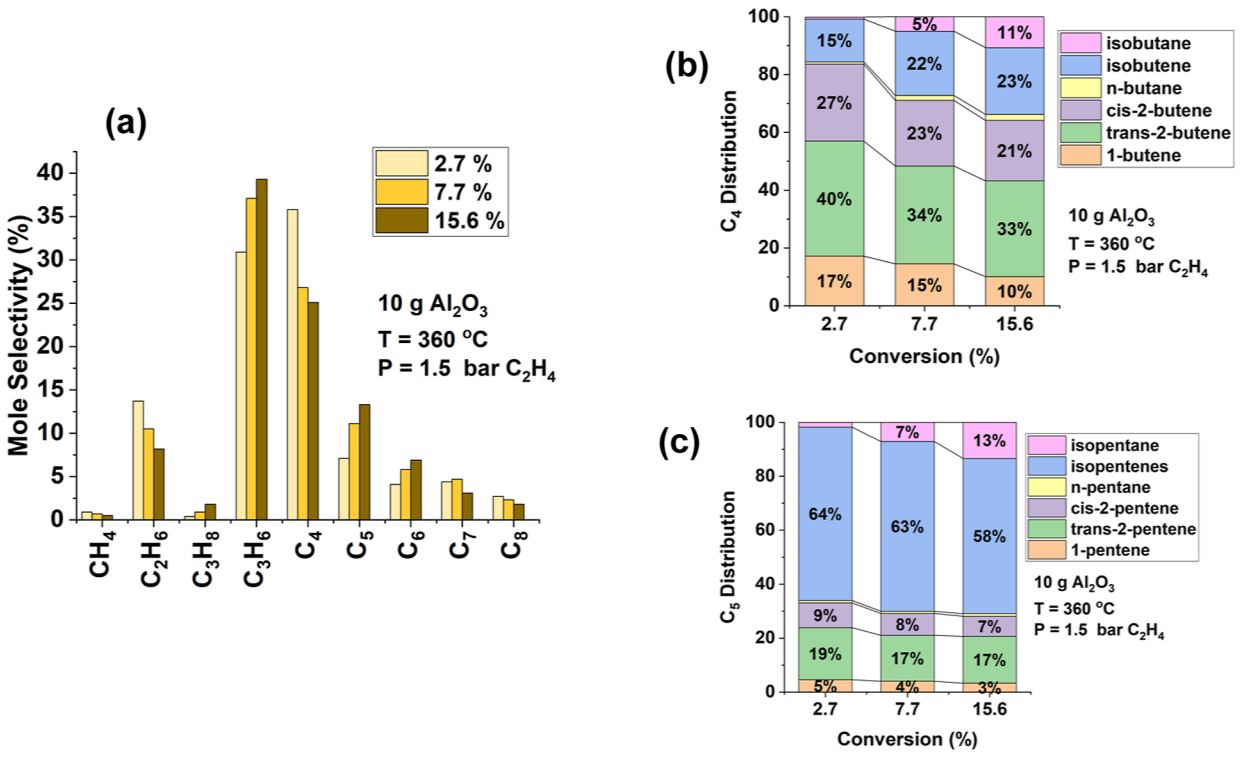

Figure 6. Products with Al_2O_3 vs conversion below 20% at 1.5 bar C_2H_4, 360 °C. (a) Carbon number distribution, (b) C_4 distribution, and (c) C_5 distribution.

selectivities were 42% 1-pentene, 31% isopentenes, and 25% 2-pentenes. *n*-Pentane was also only observed thermally, ca. 3% of C_5.

3.4. Molecular-Weight and Isomer Distributions versus Conversion. At 1.5 bar and 360 °C, the conversion varied from 2.7 to 15.6% (Figure 6). The products with increasing conversion led to increased selectivity for propylene, C_5, and C_6; decreased selectivity in C_4; and a slight decrease in ethane, C_7, and C_8 selectivities. Importantly, C_4's decreased from about 35 to 25%, whereas C_5's increased from 7 to 13% and C_6's from 3 to 7%. The propylene selectivity increased from 31 to about 40%. The ethane selectivity decreased from 14 to 8%. However, the propane selectivity increased slightly from <0.5 to 2%.

Increasing conversion also led to increased C_4 and C_5 branching, as well as increased hydrogen transfer among branched products, Figure 6b,c. The C_4 distribution, which is mostly 2-butenes (50−70%), decreases with increasing conversion, while the isobutene selectivity increases with conversion from 15 to 23% as the conversion increases from 2.7 to 15.6%. The isobutane selectivity also increases with increasing conversion from trace levels to 11%. The selectivity of *n*-butane also increases but is much lower than that of isobutane. The ratio of isobutene to isobutane decreased from >50 at 2.7% conversion to 2.1 at 15.6%. The C_5 isomers reveal similar trends to the C_4 isomers as the conversion increased, that is, the selectivity of all isopentane and isopentene products increases from 64 to 73%. Similar to the C_4's, the isopentane selectivity increases with increasing conversion, and the isopentene to isopentane ratio decreases from >50 to 4.5. *n*-Pentane selectivities remain low over this conversion range. There appeared to be at least 20 C_6 isomers products suggesting that there are skeletal isomers in the higher MW products. Less than about 5% of the C_6 is 1-hexene, which is comparable to the amount of terminal, linear C_4 and C_5.

3.5. Selectivity versus Temperature. Above 400 °C, a transition occurs toward decomposition products (methane, ethane, and coke) with alumina. As seen in Figure S1, the selectivity to methane increased from less than 1% at 300 °C to 14% at 470 °C. Likewise, the ethane selectivity increased from 8 to 47%. The remaining products are mostly propylene and C_4 with less than 3% each of C_5 to C_7. The high selectivity for saturated products was accompanied by blackening of the Al_2O_3 at 470 °C, indicating coke deposition. For comparison, at 300 °C, the Al_2O_3 remained white.

At lower temperatures, less ethane and more C_4 were formed (see Figure 7). The propylene and C_{5+} showed more complex trends, highlighting the role that consecutive olefin reactions play at different temperatures (300 and 360 °C). For example, the propylene selectivity appears the same at both temperatures until about 8% conversion; above 8% conversion, more propylene forms at 360 °C. Likewise, the C_{5+} selectivity is nearly the same at both temperatures above 8% conversion but is higher at 360 °C below 8% conversion.

Lower temperatures also led to less C_4 and C_5 branching but more hydrogen transfer among C_4 and C_5 products. Less isobutene was produced at 300 °C compared to 360 °C, as seen in Figure S2. The 60 °C decrease in reaction temperature led to about half as much isobutene (11 vs 22% of C_4). The ratio of isobutane to isobutene increased from 0.23 to 0.45. Likewise, the branched C_5 decreased from 70 to 65%, and the ratio of isopentane to isopentenes increased from 0.11 to 0.23.

3.6. Selectivity versus Pressure. The effects of pressure on the product selectivity at 1.5 versus 23 bar at 360 °C are shown in Figure 8. Ethane and propylene show the simplest pressure dependences. The ethane selectivity at 23 bar is almost double that at 1.5 bar, whereas at higher pressure, half

https://doi.org/10.1021/acs.iecr.2c02759
Ind. Eng. Chem. Res. 2023, 62, 4840−4850

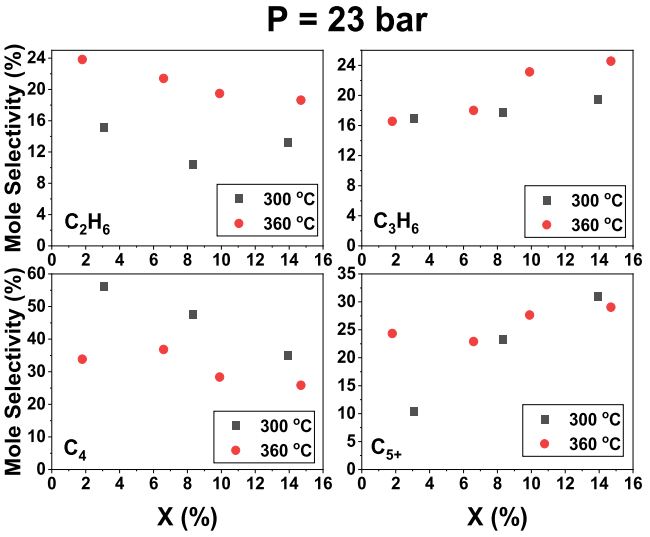

Figure 7. Selectivity of major products with Al_2O_3 at 300 vs 360 °C at 23 bar of C_2H_4 below 20% conversion.

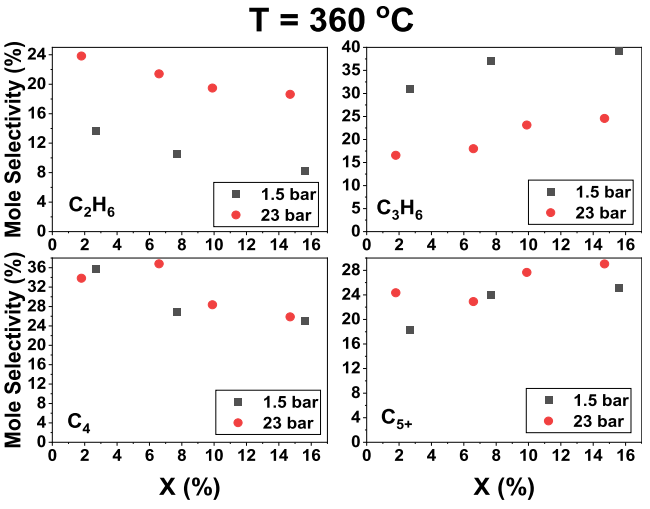

Figure 8. Selectivity of major products at 1.5 vs 23 bar of C_2H_4 at 360 °C below 20% conversion (X %).

as much propylene is produced compared to lower pressure. Both the C_4 and C_{5+} products appear in comparable amounts at both pressures.

The product distributions at 43 bar are consistent with oligomerization and hydrogen transfer as the main reactions. The even carbon oligomers (C_4, C_6, and C_8) are more abundant than the C_3, C_5, C_7, and C_9 nonoligomers with fewer nonoligomer olefins, which are present at lower pressures. For example, at 43 bar and about 8% conversion (Figure S3), the propylene selectivity is 38% at 1.5 bar but only 12% at 43 bar. The C_4 selectivity was 27% at 1.5 bar but 40% at 43 bar. Similarly, there were almost twice as many C_6 products at 43 bar.

3.7. Reaction of Propylene with Al_2O_3. The changing product distributions of ethylene with conversion, temperature, and pressure indicate that secondary reactions play an important role, and propylene was one of the products at low conversion under many temperature and pressure conditions. For ethylene conversions at 23 bar and 360 °C, propylene, for example, increased to a maximum selectivity below 20% conversion, see Figure 4, and then decreased as the conversion increased to 70%. Since propylene undergoes secondary reactions, the kinetics and products for propylene conversion with Al_2O_3 were obtained to better understand the influence of these secondary products on the rate, selectivity, and reactions.

The propylene oligomerization rate on alumina was ~10× higher than ethylene. The temperature dependence on the rate for propylene conversion with Al_2O_3 was determined from 260 to 300 °C at 1.5 bar, and the Arrhenius plot is shown in Figure 9. Over this temperature range, the apparent activation energy

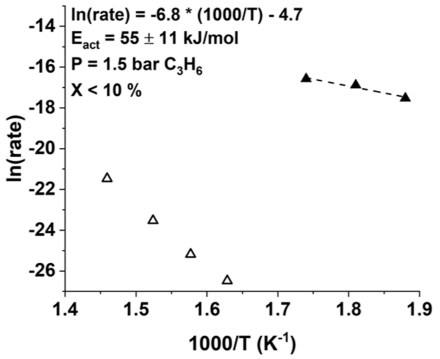

Figure 9. Kinetics of C_3H_6 reactions with Al_2O_3. Arrhenius plot from 260 to 300 °C of 1.5 bar C_3H_6. Conversions <10% the thermal reaction of C_3H_6 from 400 to 500 °C are shown in open triangles for comparison.

was 55 kJ/mol, the same as ethylene (Table S2). The conversion of C_3H_6 at 300 °C and 1.5 bar was 7.4% at a GHSV of 61 h^{-1}. For comparison, at the same conditions, the C_2H_4 conversion was 0.85% at a GHSV of 20 h^{-1}. Thus, propylene reacts about an order of magnitude faster than ethylene at 300 °C and 1.5 bar. Since propylene is one of the main products below about 20% ethylene conversion, the observed products will result from the conversion of both ethylene and propylene.

Isobutene was a major product of the reaction of propylene with alumina. At temperatures from 260 to 300 °C at 1.5 bar, the products suggest that a disproportionation reaction has occurred. The product distribution at 2.0% conversion at 260 °C in Figure 10 shows that ethylene and isobutene are the main products, comprising 27 and 28% of the products, respectively, followed by C_6 (23%). Propane was about 4%, while neither methane nor ethane was detected. Linear butenes, C_5, C_7, and C_8 products were also formed (<5% each). C_5 was mostly linear in contrast to the C_4's. Of the C_5's, only about 10% were isopentenes and 81% were 2-pentenes. The C_6 isomers consist of more than 20 distinct isomers, suggesting that they are highly branched. A comparison of the C_6 isomer products for C_3H_6 to C_2H_4 at roughly the same reaction conditions shows that the selectivities are nearly identical.

Increasing the temperature resulted in higher selectivity of C_4, C_5, and C_7 products with lower selectivities to C_2H_4 and C_6's. The effects of increasing temperature from 260 to 300 °C, shown in Figure S4 and Table S3, gave less ethylene and C_6 and more C_4. The C_4's show a gradual increase in *n*-butenes compared to isobutene at higher temperatures. Isobutene decreased from 78 to 73% of C_4, while *n*-butenes increased from 16 to 20% at higher temperatures. The isopentene selectivity increased from 15% of C_5's at 260 °C to 31% at 300 °C.

https://doi.org/10.1021/acs.iecr.2c02759
Ind. Eng. Chem. Res. 2023, 62, 4840−4850

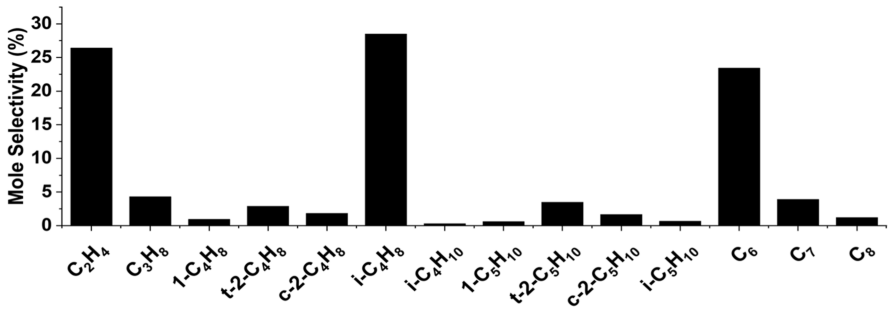

Figure 10. Products of C_3H_6 with Al_2O_3 at 2.0% conversion 260 °C and 1.5 bar.

With increasing conversion from 7.4 to 25.2% at 300 °C, the selectivities of C_4, C_5, and C_7 increased while those of C_2H_4, C_3H_8, and C_6's decreased, Figure S4. For example, ethylene and C_6 decreased from about 20 to 15 mol %, while C_4, C_5, and C_7 increased. The net increase in C_4 appears to be largely due to an increase in isobutane and *n*-butenes as opposed to the major product, isobutene. The isobutene to isobutane ratio decreased with increasing conversion, from 45 to 13. Likewise, the *iso*-pentene to isopentane ratio decreased from 87 to 22. Both *n*-butane and *n*-pentane were less than 0.2% of their respective carbon groups across the whole range of conversions. The *iso*-pentene selectivity increased from 25% of C_5 at 7.4% conversion to 36 at 25.2% conversion.

4. DISCUSSION

4.1. Catalysis of Olefins by Lewis Acid Sites on Alumina. The product distribution and kinetics of the noncatalytic, thermal olefin reactions from 300 to 500 °C were recently reported.[42] In this follow-up study, we show that olefin reactions with γ-alumina lead to significantly higher reaction rates, lower activation energies, and altered product distributions. The comparison of alumina to silica, the latter of which has a rate slightly higher than that of the empty reactor, shows that a high surface area alone does not account for the high ethylene conversion rate of the former. For example, the alumina was 270 times more active per m^2 than silica at 340 °C and 43 bar (see Table 1). The activation energies and reaction orders were also different for alumina compared to silica and the gas phase. For example, the activation energy of ethylene at 1.5 bar and 340 °C is 55 kJ/mol for alumina, 89 kJ/mol for silica, and 244 kJ/mol for the thermal reaction (Table S2). At 43 bar, the same trend was observed; the activation energy for alumina (76 kJ/mol) was much lower than that for silica (176 kJ/mol) and the noncatalytic, gas-phase reaction (244 kJ/mol). The reaction rates at 1.5 and 43 bar also lead to different apparent reaction orders for silica (1.4) and alumina (1.1), which are both less than the gas-phase reaction order of 1.9. The significantly higher reaction rates, different activation energies, reaction order, and altered product distributions indicate that alumina is catalytic for the conversion of olefins to higher molecular weight products at temperatures above about 250 °C and especially at pressures greater than about 20 bar.

The Sasol Sba alumina in this study has both tetrahedral, ca. 23% at 78 ppm, and octahedral, ca. 77% at 9 ppm, Al coordination sites by ^{27}Al MAS NMR, Figure S5a. The peaks in the IR spectra of adsorbed pyridine near 1589 and 1445 cm^{-1}, Figure S5b, are characteristic of Lewis acid sites.[62,73,74] Additionally, there are no peaks in the IR spectra at 1540 cm^{-1} due to Bronsted acid sites.[73] Compared to the gas-phase thermal products, the alumina C_4 and C_5 isomer distributions show greater selectivity toward double bond isomerization, branching, and H-transfer products. Silica, which has neither Lewis nor Bronsted acid sites,[73] gave essentially the same product distribution to the empty reactor suggesting the importance of the Lewis acid sites in the catalytic conversions. These results are also consistent with observations by Lucchesi et al. that alumina adsorbs ethylene but not silica.[75,76]

4.2. Comparison of the Ethylene Reaction Products for Noncatalytic Thermal and Alumina Catalytic Conversions. In addition to differences in kinetics, there are also differences in the reaction products of noncatalytic, thermal, and alumina-catalyzed olefin reactions. While non-oligomer products were present at all reaction conditions with Al_2O_3, analogous to the thermal reaction, alumina dimerization is favored at low conversion of ethylene and high pressure. This selectivity decreases at higher conversions and lower pressures, and the molecular distribution is similar to that of the gas-phase reactions. The nonoligomer products suggest fragmentation pathways for higher molecular weight products. For alumina, this develops as early as 2.7% conversion at 360 °C and 1.5 bar (see Figure 6a).

The thermal reactions produce a high fraction of 1-butene (69%) and 1-pentene (42%) (see Figure 5b,c); however, with alumina, 1-butene and 1-pentene selectivities are lower, 25 and 7%, respectively. This observation is consistent with the fact that alumina is a well-known double bond and cis/trans olefin isomerization catalyst, which is generally attributed to Lewis acid sites.[47,48,52,55] Branched C_4 and C_5 were present at all conversions with alumina but were not major products for thermal reactions. On alumina at low conversions (e.g. Figure 5b,c), isobutene was a minor C_4 isomer (about 4%) but became significant (>20%) at higher conversions, suggesting that it forms by secondary reactions of the primary products. Lastly, more than 20 C_6 isomers were detected, which indicates that C_6 is also highly branched.

Isobutene appears to be formed from the secondary reaction of propylene, Figure 10 (and Section 4.3 below for the reaction of propylene); however, it is not known how this reaction occurs on alumina. The skeletal isomerization of linear butenes is well known for Brønsted acid catalysts, for example, with zeolites, via sequential oligomerization, skeletal isomerization, and cracking.[77,78] However, γ-Al_2O_3 lacks Brønsted acid sites and is not known to catalyze skeletal isomerization or have high cracking activity.[57,60−62]

Another distinguishing feature of the reactions of ethylene with alumina compared to the gas phase was the production of a modest selectivity to ethane (ca. 5−20 mol %), which was very low (<1 mol %) in the absence of alumina. At higher ethylene conversion where the products included isobutene and isopentenes, the selectivity to isobutane and isopentane

https://doi.org/10.1021/acs.iecr.2c02759
Ind. Eng. Chem. Res. 2023, 62, 4840−4850

increased. These shifts to saturated, higher molecular weight products occurred concurrently with a decreasing selectivity to ethane. This "self-hydrogenation" phenomenon was reported by Hindin and Weller previously at low ethylene pressures in the absence of significant oligomerization and ascribed to highly strained Lewis acid sites formed by dehydration of the surface.[49]

The production of saturated products without cofeeding hydrogen also requires other products with fewer hydrogens. However, no C_2 to C_4 products with multiple degrees of unsaturation (e.g., acetylene, propadiene, and butadiene) were detected below 400 °C, suggesting that the unsaturated species were C_{5+} products. Because of the many reaction products at high conversion, these have not been identified. The ethylene conversion rates were stable over several days, and the alumina did not appear to form coke or become black below about 400 °C. For example, after the reaction at 360 °C, the used catalyst was light orange, suggesting oligomeric surface adsorbates. However, these do not lead to a significant loss of activity even at 70% conversion.

In summary, many of the product differences between thermal (noncatalytic) and catalytic reactions on alumina can be accounted for by secondary reactions, for example, double bond isomerization and hydrogen transfer, by Lewis sites on alumina. In addition, alumina catalyzes olefin oligomerization at much higher rates than those for thermal conversions.

4.3. Propylene Disproportionation and Lower Rate of H-Transfer by C_3H_6 with Al_2O_3. The reaction of propylene with alumina gives rise to a lower selectivity of dimers and a lower extent of H-transfer than for ethylene. The main products at low conversion are not simply dimer products (C_6) but also disproportionation products (ethylene and isobutene) (e.g., Figure 10). The latter products are significantly different from those due to the thermal reaction of propylene, where propylene has a high selectivity (>70%) for dimeric C_6 products at 400 °C.[42] For alumina, the selectivity to form oligomeric products was <30%. With alumina, even at 260 °C, the dimer is the minor product (ca. 25%) compared to isobutene, ethylene, and other non-C_6 products (see Figure 10). The production of equivalent amounts of ethylene and isobutene from propylene at low conversion is not consistent with Brønsted acid sites, suggesting that the Lewis acid sites are responsible. For example, the reaction of propylene with H-ZSM-5 at 250 °C has been shown to produce *i*-C_4 and *i*-C_5 cracking products in stoichiometric amounts below 4% conversion, which was ascribed to the cracking of C_9 oligomers.[78] Furthermore, no ethylene was reported from propylene with H-ZSM-5 in that study.

The reaction of propylene with alumina also gives a lower selectivity of saturated products compared to ethylene. For example, the ethane selectivity was about 10 mol % at about 5−10% ethylene conversion (see Figure S2), whereas propane was only about 5 mol % at low conversions of propylene (see Figure S4). This result is different than that for the thermal reactions of ethylene and propylene, where propylene produced more saturated products (methane, ethane, and propane). The higher reactivity of vinyl bonds versus allylic bonds on alumina is in good agreement with the higher rates of D_2 exchange of ethylene than propylene.[70,71] In addition, on alumina, the rate of D_2 exchange with propylene at room temperature was the highest for the unsubstituted, followed by the substituted vinyl hydrogens, while allylic hydrogen had the lowest rate.[72] Thus, the higher selectivity of ethylene for saturated products in this study is consistent with the higher ethylene−D_2 isotope exchange rates of ethylene than for propylene.

5. CONCLUSIONS

At reaction temperatures above about 250 °C and pressures from 1 to 40 bar, olefins react on alumina to form higher molecular weight products. The rate of propylene is about ten times higher than that of ethylene. The products are not a simple olefin oligomerization distribution, and many non-oligomer products are formed. The primary products undergo secondary double bond isomerization; however, skeletal isomerization does not appear to occur. Additional secondary reactions also include H-transfer, leading to saturated products. Some reactants and products undergo disproportionation reactions; for example, propylene forms equal molar amounts of ethylene and *iso*-butene at low conversions. While H−D isotopic exchange and double-bond isomerization of olefins are known reactions on alumina, olefin oligomerization and disproportionation have not been previously reported.

Similar to many previous studies of alumina, the Sasol Sba alumina has only Lewis acid sites. The latter have been previously proposed to be the active site for double bond isomerization and H−D exchange. Thus, it seems likely that Lewis acid sites are also catalytic for olefin oligomerization and disproportionation reactions. The reaction intermediates and pathways for olefin oligomerization and disproportionation on alumina are not known. In addition, it is not known how the nonoligomer products are formed. Secondary reactions of the disproportionation products with the reactants may account for the nonoligomeric products; however, other pathways are also possible.

■ ASSOCIATED CONTENT

Supporting Information

The Supporting Information is available free of charge at https://pubs.acs.org/doi/10.1021/acs.iecr.2c02759.

Olefin conversion rates and kinetics, olefin reaction product distributions with Al_2O_3, sample GC chromatograms, and Al MAS NMR and IR spectra of adsorbed pyridine (PDF)

■ AUTHOR INFORMATION

Corresponding Author

Jeffrey T. Miller − *Davidson School of Chemical Engineering, Purdue University, West Lafayette, Indiana 47907, United States;* orcid.org/0000-0002-6269-0620; Email: jeffrey-t-miller@purdue.edu

Authors

Matthew A. Conrad − *Davidson School of Chemical Engineering, Purdue University, West Lafayette, Indiana 47907, United States*

Jaiden E. DeLine − *Davidson School of Chemical Engineering, Purdue University, West Lafayette, Indiana 47907, United States*

Complete contact information is available at: https://pubs.acs.org/10.1021/acs.iecr.2c02759

Notes

The authors declare no competing financial interest.

https://doi.org/10.1021/acs.iecr.2c02759
Ind. Eng. Chem. Res. 2023, 62, 4840−4850

■ ACKNOWLEDGMENTS

This paper is based upon work supported primarily by the National Science Foundation (NSF) under Cooperative Agreement no. EEC-1647722. Any opinions, findings, conclusions, or recommendations expressed in this material are those of the author(s) and do not necessarily reflect the views of the National Science Foundation. The authors would like to thank John Harwood from the Purdue Interdepartmental NMR Facility in the Department of Chemistry for obtaining the Al NMR MAS spectra. The authors would also like to thank Christian Breckner and Sopuruchukwu Ezenwa in the Davison School of Chemical Engineering for obtaining the IR spectra of adsorbed pyridine on alumina.

■ REFERENCES

(1) Bell, A. T.; Alger, M. M.; Flytzani-Stephanopoulos, M.; Gunnoe, T. B.; Lercher, J. A.; Stevens, J.; Alper, J.; Tran, C. *The Changing Landscape of Hydrocarbon Feedstocks for Chemical Production: Implications for Catalysis: Proceedings of a Workshop; 1344369*; National Academies Press, 2016; p 1344369.
(2) Ridha, T.; Li, Y.; Gençer, E.; Siirola, J.; Miller, J.; Ribeiro, F.; Agrawal, R. Valorization of Shale Gas Condensate to Liquid Hydrocarbons through Catalytic Dehydrogenation and Oligomerization. *Processes* **2018**, *6*, 139.
(3) Nalley, S.; LaRose, A. *Annual Energy Outlook 2021*; Press Release; Washington, D.C., 2021.
(4) Pillai, S. M.; Ravindranathan, M.; Sivaram, S. Dimerization of Ethylene and Propylene Catalyzed by Transition-Metal Complexes. *Chem. Rev.* **1986**, *86*, 353−399.
(5) O'Connor, C. T.; Kojima, M. Alkene Oligomerization. *Catal. Today* **1990**, *6*, 329−349.
(6) Skupinska, J. Oligomerization of .alpha.-olefins to higher oligomers. *Chem. Rev.* **1991**, *91*, 613−648.
(7) Al-Jarallah, A. M.; Anabtawi, J. A.; Siddiqui, M. A. B.; Aitani, A. M.; Al-Sa'doun, A. W. Ethylene dimerization and oligomerization to butene-1 and linear α-olefins. *Catal. Today* **1992**, *14*, 1−121.
(8) Forestière, A.; Olivier-Bourbigou, H.; Saussine, L. Oligomerization of Monoolefins by Homogeneous Catalysts. *Oil Gas Sci. Technol.* **2009**, *64*, 649−667.
(9) McGuinness, D. S. Olefin Oligomerization via Metallacycles: Dimerization, Trimerization, Tetramerization, and Beyond. *Chem. Rev.* **2011**, *111*, 2321−2341.
(10) Sydora, O. L. Selective Ethylene Oligomerization. *Organometallics* **2019**, *38*, 997−1010.
(11) Olivier-Bourbigou, H.; Breuil, P. A. R.; Magna, L.; Michel, T.; Espada Pastor, M. F.; Delcroix, D. Nickel Catalyzed Olefin Oligomerization and Dimerization. *Chem. Rev.* **2020**, *120*, 7919−7983.
(12) Finiels, A.; Fajula, F.; Hulea, V. Nickel-based solid catalysts for ethylene oligomerization - a review. *Catal. Sci. Technol.* **2014**, *4*, 2412−2426.
(13) Nicholas, C. P. Applications of Light Olefin Oligomerization to the Production of Fuels and Chemicals. *Appl. Catal., A* **2017**, *543*, 82−97.
(14) Ghashghaee, M. Heterogeneous Catalysts for Gas-Phase Conversion of Ethylene to Higher Olefins. *Rev. Chem. Eng.* **2018**, *34*, 595−655.
(15) Schmerling, L.; Ipatieff, V. N. The Mechanism of the Polymerization of Alkenes. *Adv. Catal.* **1950**, *2*, 21−80.
(16) Jones, E. K. Polymerization of Olefins from Cracked Gases. *Adv. Catal.* **1956**, *8*, 219−238.
(17) Oblad, A. G.; Mills, G. A.; Heinemann, H. Polymerization of Olefins (to Liquid Polymers). In *Catalysis*; Reinhold Publishing Corporation, 1958; Vol. *6*.
(18) Corma, A.; Iborra, S. Oligomerization of Alkenes. In *Catalysts for Fine Chemical Synthesis*; Derouane, E. G., Ed.; John Wiley & Sons, Ltd: Chichester, U.K., 2006; pp 125−140.
(19) Sanati, M.; Hörnell, C.; Järäs, S. G. The Oligomerization of Alkenes by Heterogeneous Catalysts. In *Catalysis*; Spivey, J. J., Ed.; Royal Society of Chemistry: Cambridge, 2007; Vol. *14*, pp 236−288.
(20) Mehlberg, R. L.; Pujadó, P. R.; Ward, D. J. Olefin Condensation. In *Handbook of Petroleum Processing*; Treese, S. A., Pujadó, P. R., Jones, D. S. J., Eds.; Springer International Publishing: Cham, 2015; pp 457−478.
(21) Antunes, B. M.; Rodrigues, A. E.; Lin, Z.; Portugal, I.; Silva, C. M. Alkenes Oligomerization with Resin Catalysts. *Fuel Process. Technol.* **2015**, *138*, 86−99.
(22) Frolich, P. K.; Wiezevich, P. J. Symposium on the Chemistry of Gaseous Hydrocarbons Cracking and Polymerization of Low Molecular Weight Hydrocarbons. *Ind. Eng. Chem.* **1935**, *27*, 1055−1062.
(23) Wagner, C. R. Production of Gasoline by Polymerization of Olefins. *Ind. Eng. Chem.* **1935**, *27*, 933−936.
(24) Maschwitz, P. A.; Henderson, L. M. Polymerization of Hydrocarbon Gases to Motor Fuels. In *Progress in Petroleum Technology*; Advances in Chemistry; American Chemical Society, 1951; Vol. *5*, pp 83−96.
(25) Asinger, F. The Working Up of Lower, Normally Gaseous Paraffins and Mono-Olefins to Give Carburettor Fuels. In *Mono-Olefins*; Elsevier, 1968; pp 414−505.
(26) Egloff, G.; Schaad, R. E.; Lowry, C. D. Decomposition and Polymerization of the Olefinic Hydrocarbons. *J. Phys. Chem.* **1931**, *35*, 1825−1903.
(27) Stanley, H. M. The Polymerisation Reactions of Ethylene. *J. Soc. Chem. Ind.* **1930**, *49*, T349−T354.
(28) Yamada, B.; Zetterlund, P. B. General Chemistry of Radical Polymerization. In *Handbook of Radical Polymerization*; Matyjaszewski, K., Davis, T. P., Eds.; John Wiley & Sons, Inc.: Hoboken, NJ, USA, 2002; pp 117−186.
(29) Elias, H.-G. Free-Radical Polymerization. In *Macromolecules*; Wiley-VCH Verlag GmbH: D-69451 Weinheim, Germany, 2014; pp 309−367.
(30) Peuckert, M.; Keim, W. A New Nickel Complex for the Oligomerization of Ethylene. *Organometallics* **1983**, *2*, 594−597.
(31) Lutz, E. F. Shell Higher Olefins Process. *J. Chem. Educ.* **1986**, *63*, 202.
(32) Keim, W. Nickel: An Element with Wide Application in Industrial Homogeneous Catalysis. *Angew. Chem., Int. Ed. Engl.* **1990**, *29*, 235−244.
(33) Freitas, E. R.; Gum, C. R. Shell's Higher Olefins Process. *Chem. Eng. Prog.* **1979**, *75*, 73−76.
(34) Andrews, J.; Bonnifay, P. The IFP Dimersol Process for Dimerization of Propylene into Isohexenes. In *ACS Symposium Series*; American Chemical Society, 1977; pp 328−340.
(35) Al-Sherehy, F. A. IFP-SABIC Process for the Selective Ethylene Dimerization to Butene-1. *Stud. Surf. Sci. Catal.* **1996**, *100*, 515−523.
(36) Manyik, R. A Soluble Chromium-Based Catalyst for Ethylene Trimerization and Polymerization. *J. Catal.* **1977**, *47*, 197−209.
(37) McGuinness, D. S.; Wasserscheid, P.; Keim, W.; Hu, C.; Englert, U.; Dixon, J. T.; Grove, C. Novel Cr-PNP Complexes as Catalysts for the Trimerisation of Ethylene. *Chem. Commun.* **2003**, 334−335.
(38) Ziegler, K. Aluminium-organische Synthese im Bereich olefinischer Kohlenwasserstoffe. *Angew. Chem.* **1952**, *64*, 323−329.
(39) Shiraki, Y.; Kawano, S.; Takeuchi, K. Process For Preparing Linear A-Olefins. U.S. Patent 4,783,573 A, November 8, 1988.
(40) Sullivan, F. W.; Ruthruff, R. F.; Kuentzel, W. E. Pyrolysis and Polymerization of Gaseous Paraffins and Olefins. *Ind. Eng. Chem.* **1935**, *27*, 1072−1077.
(41) Egloff, G. Polymer Gasoline. *Ind. Eng. Chem.* **1936**, *28*, 1461.
(42) Conrad, M. A.; Shaw, A.; Marsden, G.; Broadbelt, L. J.; Miller, J. T. Insights into the Chemistry of the Homogeneous Thermal Oligomerization of Ethylene to Liquid-Fuel-Range Hydrocarbons. *Ind. Eng. Chem. Res.* **2023**, *62*, 2202.

https://doi.org/10.1021/acs.iecr.2c02759
Ind. Eng. Chem. Res. 2023, 62, 4840−4850

(43) Greensfelder, B. S.; Voge, H. H.; Good, G. M. Catalytic and Thermal Cracking of Pure Hydrocarbons: Mechanisms of Reaction. *Ind. Eng. Chem.* **1949**, *41*, 2573−2584.
(44) Ipatieff, V. N. Catalytic Reactions at High Temperatures and Pressures. *Chem. Zentralbl.* **1906**, *2*, 86.
(45) Ipatieff, V. N. Catalytic Reactions at High Pressures and Temperatures: Influence of Pressure on the Course of Catalysis. *Zh. Russ. Fiz.-Khim.* **1906**, *38*, 63−75.
(46) Brey, W. S.; Krieger, K. A. The Surface Area and Catalytic Activity of Aluminum Oxide. *J. Am. Chem. Soc.* **1949**, *71*, 3637−3641.
(47) Oblad, A. G.; Messenger, J. U.; Brown, H. T. Isomerization of 1- and 2-Pentenes. *Ind. Eng. Chem.* **1947**, *39*, 1462−1466.
(48) Naragon, E. A. Catalytic Isomerization of 1-Hexene. *Ind. Eng. Chem.* **1950**, *42*, 2490−2493.
(49) Hindin, S. G.; Weller, S. W. The Effect of Pretreatment on the Activity of Gamma-Alumina. I. Ethylene Hydrogenation. *J. Phys. Chem.* **1956**, *60*, 1501−1506.
(50) Hindin, S. G.; Weller, S. W. 10 Catalysis of Ethylene Hydrogenation and Hydrogen-Deuterium Exchange by Dehydrated Alumina. *Adv. Catal.* **1957**, *9*, 70−75.
(51) Pines, H.; Haag, W. O. Alumina: Catalyst and Support. I. Alumina, its Intrinsic Acidity and Catalytic Activity1. *J. Am. Chem. Soc.* **1960**, *82*, 2471−2483.
(52) Brouwer, D. The Mechanism of Double-Bond Isomerization of Olefins on Solid Acids. *J. Catal.* **1962**, *1*, 22−31.
(53) Sinfelt, J. H. Kinetics of Ethylene Hydrogenation over Alumina. *J. Phys. Chem.* **1964**, *68*, 232−237.
(54) Corado, A. Catalytic isomerization of olefins on alumina *1II. Catalyst deactivation and its effects on the mechanism. *J. Catal.* **1975**, *37*, 68−80.
(55) Medema, J. Isomerization of butene over alumina*1. *J. Catal.* **1975**, *37*, 91−100.
(56) Butler, A. C.; Nicolaides, C. P. Catalytic Skeletal Isomerization of Linear Butenes to Isobutene. *Catal. Today* **1993**, *18*, 443−471.
(57) Rodemerck, U.; Kondratenko, E. V.; Otroshchenko, T.; Linke, D. Unexpectedly High Activity of Bare Alumina for Non-Oxidative Isobutane Dehydrogenation. *Chem. Commun.* **2016**, *52*, 12222−12225.
(58) Zhao, D.; Lund, H.; Rodemerck, U.; Linke, D.; Jiang, G.; Kondratenko, E. V. Revealing fundamentals affecting activity and product selectivity in non-oxidative propane dehydrogenation over bare Al2O3. *Catal. Sci. Technol.* **2021**, *11*, 1386−1394.
(59) Wang, P.; Xu, Z.; Wang, T.; Yue, Y.; Bao, X.; Zhu, H. Unmodified Bulk Alumina as an Efficient Catalyst for Propane Dehydrogenation. *Catal. Sci. Technol.* **2020**, *10*, 3537−3541.
(60) Rodemerck, U.; Sokolov, S.; Stoyanova, M.; Bentrup, U.; Linke, D.; Kondratenko, E. V. Influence of Support and Kind of VO Species on Isobutene Selectivity and Coke Deposition in Non-Oxidative Dehydrogenation of Isobutane. *J. Catal.* **2016**, *338*, 174−183.
(61) Busca, G. Spectroscopic Characterization of the Acid Properties of Metal Oxide Catalysts. *Catal. Today* **1998**, *41*, 191−206.
(62) Knözinger, H. A Test for the Development of Protonic Acidity in Alumina at Elevated Temperatures. *J. Catal.* **1972**, *25*, 436−438.
(63) Holm, V. C. F.; Clark, A. Catalytic Properties of Fluorine-Promoted Alumina. *Ind. Eng. Chem. Prod. Res. Dev.* **1963**, *2*, 38−39.
(64) Choudhary, V. R. Fluorine Promoted Catalysts: Activity and Surface Properties. *Ind. Eng. Chem. Prod. Res. Dev.* **1977**, *16*, 12−22.
(65) Cheng, Z.; Ponec, V. Fluorinated Alumina as a Catalyst for Skeletal Isomerization of N-Butene. *Appl. Catal., A* **1994**, *118*, 127−138.
(66) Gayubo, A. G.; LLorens, F. J.; Cepeda, E. A.; Bilbao, J. Deactivation and Regeneration of a Chlorinated Alumina Catalyst Used in the Skeletal Isomerization of n-Butenes. *Ind. Eng. Chem. Res.* **1997**, *36*, 5189−5195.
(67) Knözinger, H. Dehydration of Alcohols on Aluminum Oxide. *Angew. Chem., Int. Ed. Engl.* **1968**, *7*, 791−805.
(68) Holm, C. V. C. F.; Blue, R. W. Hydrogen-Deuterium Exchange Activity of Silica-Alumina. *Ind. Eng. Chem.* **1951**, *43*, 501−505.
(69) Larson, J. G.; Hall, W. K. Studies of the Hydrogen Held by Solids. VII. The Exchange of the Hydroxyl Groups of Alumina and Silica-Alumina Catalysts with Deuterated Methane. *J. Phys. Chem.* **1965**, *69*, 3080−3089.
(70) Larson, J. G.; Hightower, J. W.; Hall, W. K. Tracer Studies of Acid-Catalyzed Reactions. III. Preparation of Perdeuterio Olefins and Cyclopropane by Reaction with Deuterium over Alumina. *J. Org. Chem.* **1966**, *31*, 1225−1227.
(71) Hightower, J. Tracer Studies of Acid-Catalyzed Reactions IX. Exchange of D2 with Noncyclic Olefins over Alumina. *J. Catal.* **1969**, *13*, 161−168.
(72) Hughes, B. T.; Kemball, C.; Tyler, J. K. Exchange Reactions of Propene on Oxide Catalysts Investigated by Microwave Spectroscopy. *J. Chem. Soc., Faraday Trans. 1* **1975**, *71*, 1285.
(73) Parry, E. P. An Infrared Study of Pyridine Adsorbed on Acidic Solids. Characterization of Surface Acidity. *J. Catal.* **1963**, *2*, 371−379.
(74) Liu, X.; Truitt, R. E. DRFT-IR Studies of the Surface of γ-Alumina. *J. Am. Chem. Soc.* **1997**, *119*, 9856−9860.
(75) Lucchesi, P. J.; Carter, J. L.; Yates, D. J. C. An Infrared Study of the Chemisorption of Ethylene on Aluminum Oxide. *J. Phys. Chem.* **1962**, *66*, 1451−1456.
(76) Yates, D. J. C.; Lucchesi, P. J. Effects of γ-Radiation on the Surface Properties of Silica as Studied by the Infrared Spectra of Adsorbed Molecules. *J. Am. Chem. Soc.* **1964**, *86*, 4258−4265.
(77) Quann, R. J.; Green, L. A.; Tabak, S. A.; Krambeck, F. J. Chemistry of Olefin Oligomerization over ZSM-5 Catalyst. *Ind. Eng. Chem. Res.* **1988**, *27*, 565−570.
(78) Vernuccio, S.; Bickel, E. E.; Gounder, R.; Broadbelt, L. J. Microkinetic Model of Propylene Oligomerization on Brønsted Acidic Zeolites at Low Conversion. *ACS Catal.* **2019**, *9*, 8996−9008.

https://doi.org/10.1021/acs.iecr.2c02759
Ind. Eng. Chem. Res. 2023, 62, 4840−4850